

General Disclaimer

One or more of the Following Statements may affect this Document

- This document has been reproduced from the best copy furnished by the organizational source. It is being released in the interest of making available as much information as possible.
- This document may contain data, which exceeds the sheet parameters. It was furnished in this condition by the organizational source and is the best copy available.
- This document may contain tone-on-tone or color graphs, charts and/or pictures, which have been reproduced in black and white.
- This document is paginated as submitted by the original source.
- Portions of this document are not fully legible due to the historical nature of some of the material. However, it is the best reproduction available from the original submission.

NASA Technical Memorandum 72856

UTILIZATION OF THE WING-BODY AERODYNAMIC
ANALYSIS PROGRAM

Robert E. Curry

October 1978



(NASA-TM-72856) UTILIZATION OF THE
WING-BODY AERODYNAMIC ANALYSIS PROGRAM

(NASA) 29 p HC A03/MF A01

CSCL 01A

N79-10020

Unclas

G3/02 33845

NASA Technical Memorandum 72856

UTILIZATION OF THE WING-BODY AERODYNAMIC
ANALYSIS PROGRAM

Robert E. Curry

Dryden Flight Research Center
Edwards, California



National Aeronautics and
Space Administration

Scientific and Technical
Information Office

1978

UTILIZATION OF THE WING-BODY AERODYNAMIC ANALYSIS PROGRAM

Robert E. Curry
Dryden Flight Research Center

INTRODUCTION

A version of the Woodward-Carmichael panel pressure computer analysis technique used at the National Aeronautics and Space Administration Dryden Flight Research Center (NASA DFRC) has been applied to several diverse aerodynamic studies. The purpose of this paper is to document work performed with this computer program.

The program calculates the potential, inviscid, steady-state flow solution for a given wing and body combination in subsonic or supersonic flow. The program was developed at the NASA Ames Research Center using the Woodward technique. A description of this computational method is included in references 1 and 2. The latest version of the program has been in use at DFRC since 1975 and is commonly referred to as Wing-Body.

Experience gained in the use of this program includes both its intended applications as well as some unusual applications. This report presents the methods and success of using Wing-Body to determine aircraft stability and control characteristics, potential flow field characteristics, air launch dynamics, and wake vortex up-set loads. The limitations and range of application of the program are also discussed.

The greatest advantage of the Wing-Body version over most existing aerodynamic analytical techniques is that it is user oriented. Preparation of computer input is simplified by the use of many default values and an automatic paneling feature. The input scheme is also very versatile, allowing nonconventional uses of the program.

The Wing-Body analytical techniques for determining aircraft stability and control derivatives are shown to be valid. The effects of design changes can be closely predicted prior to wind tunnel and flight testing. Other analytical procedures, such as the determination of launch dynamics or wake-vortex-induced loads, provide results which cannot be easily obtained by experiment.

The analysis presented in this paper was performed by an engineering student trainee at DFRC as part of the cooperative trainee program.

SYMBOLS

The body axis system assumed throughout this report is consistent with that used by Wing-Body. X is positive in the aft direction, Y is positive to the right, and Z is positive up.

A	panel area, m^2
b	reference span, m
C_L	lift coefficient
C_ℓ	rolling moment coefficient
C_m	pitching moment coefficient
C_N	normal force coefficient
C_n	yawing moment coefficient
C_p	pressure coefficient
C_Y	side force coefficient
\bar{c}	reference chord, m
c_{B52}	chord of B-52 airplane, span station 208, m
K	number of panels
M	Mach number
n	variable
S	reference planform area, m^2
V	airspeed, m/sec
V_z	vertical velocity component, m/sec

XC	longitudinal distance from panel centroid to center of gravity, m
YC	lateral distance from panel centroid to center of gravity, m
ΔC_p	lower surface C_p minus upper surface C_p
ψ	effective twist angle, deg
Subscripts:	
BODY	contribution of the body
α	derivative with respect to angle of attack, per deg
β	derivative with respect to angle of yaw, per deg
δ_a	derivative with respect to aileron deflection, per deg
δ_e	derivative with respect to elevator deflection, per deg
δ_r	derivative with respect to rudder deflection, per deg

DESCRIPTION OF WING-BODY PROGRAM

Operation of the Wing-Body program requires that a wing or body configuration, or both, be specified in terms of trapezoidal constant pressure panels. Flow conditions, primarily angle of attack and Mach number, are also specified. Using these inputs, the program represents the wing as a surface distribution of sources and vorticity and the body as a line distribution of sources and doublets in a linearized potential flow field. The body is simulated once in axial flow and once in flow produced by the presence of the wing. The program computes the potential, steady-state pressure coefficient on each body panel and on the upper and lower surface of each wing panel. Using the differential pressure coefficient, ΔC_p , which is the difference between the C_p values for the lower and upper surfaces, the total aircraft force and moment coefficients are obtained.

The Wing-Body results are based on the potential flow equation. If subsonic flow is desired, results are obtained by the use of a coordinate system transformation based on the Prandtl-Glauert factor, which produces an equivalent configuration in incompressible flow. If supersonic flow is required, a transformed configuration at a Mach number of $\sqrt{2}$ is obtained, which is equivalent to the desired configuration and Mach number. The results are then adjusted to the desired Mach number. Use of the program in the transonic region is not valid because of viscous effects that position the embedded shock waves. The suggested range of application is therefore subsonic or supersonic ($M = 0$ to 0.85 or $M = 1.5$ to 3.0). Wing-Body does not account for nonlinear flow conditions such as vortex formation or flow

separation and stall. Therefore, coefficients derived using Wing-Body will always be linear with respect to angle of attack, regardless of the type of flow actually experienced by the aircraft.

The severest limitation of this version of the Woodward-Carmichael method has been the number of panels that can be used. Wing surface description is limited to 100 panels. Other versions accept the use of more panels but generally require substantially more computer time. For symmetric configurations, Wing-Body allows the entire number of panels to be used to represent one-half of the configuration. The resulting coefficients are then doubled.

The leading and trailing edges of each panel may be swept; however, the two side edges must be parallel to the free stream. Triangular panels are acceptable if a streamwise side is set equal to zero. Dihedral, camber, and thickness may also be specified for each panel. Camber inputs are equivalent to the local angle of attack of each panel. When describing a computer model, it is important that all wing surfaces be subdivided into panels at the same span stations so that the panels along any streamwise row will have the same width and their streamwise side edges will coincide.

The program incorporates several features that reduce the input preparation time. Data are arranged in namelist form for which most variables have default values. Except for angular values, no specific unit system is required because all results are nondimensionalized. Another feature automatically divides wing surfaces into the desired number of spanwise and chordwise panels. The paneling of the fuselage, including forebody and afterbody closures, is performed internally. A plotting routine is available that allows verification of the paneling scheme input by the user.

On the CDC Cyber 70, Model 73, Wing-Body (without overlay) requires 177,000 octal words of central memory, and most cases take less than three minutes of central processor time.

CONFIGURATION STABILITY ANALYSIS

Static stability derivatives of flight vehicles can be evaluated by Wing-Body with respect to angle of attack, sideslip, or control surface deflections. The following set of stability and control derivatives can be accurately determined: C_{L_α} , C_{m_α} , $C_{L_{\delta_e}}$, $C_{\ell_{\delta_a}}$, $C_{n_{\delta_a}}$, C_{n_β} , C_{Y_β} , $C_{\ell_{\delta_r}}$, and $C_{Y_{\delta_r}}$. Drag coefficients are

only first-order approximations and are not suitable to evaluate vehicle performance. When appropriate, as in the case of oblique wing vehicles, terms such as rolling moment due to elevator, $C_{\ell_{\delta_e}}$, or pitching moment due to aileron, $C_{m_{\delta_a}}$, can

be obtained.

The F-111 transonic aircraft technology (TACT) research airplane was analyzed by the use of the method. Stability changes resulting from wing sweep angle and Mach number variations were determined and the results compared favorably with the flight data included in reference 3.

Five computer passes and three computer models were required to obtain a complete set of derivatives. To obtain derivatives with respect to angle of attack, sideslip, elevator deflection, aileron deflection, and rudder deflection, a separate computer pass was required for each case. The three models are shown in figure 1 and represent only the TACT aircraft's planform. Wing thickness and camber do not affect the desired results. The paneling scheme was purposely arranged such that groups of panels correspond in location and size to control surfaces. Camber was then added to these control surface panels and the resulting incremental changes in aircraft forces and moments indicate the control surface effectiveness.

The program tends to overpredict the effect of camber inputs near the trailing edge. Therefore, when analyzing conventional trailing edge control surfaces, the control derivatives obtained are usually multiplied by a scale factor of 2/3. No scale factor is required when the control surface under consideration consists of an all-movable wing surface. The TACT aircraft has both types of control surfaces, the rudder being a conventional trailing edge device, with the computed results being adjusted accordingly, and the aileron and elevator control being provided by the all-moving horizontal stabilizer which required no adjustment.

The first model (fig. 1(a)) was used to determine the longitudinal derivatives. The symmetric configuration option was employed, and, therefore, all the available panels could be used to represent one-half of the aircraft. Vertical surfaces were not modeled.

The second model (fig. 1(b)) was used to estimate lateral derivatives. The asymmetric option was used here so that differential camber inputs could be made to the aileron panels. Because of this, the paneling was much coarser for this model. Only derivatives with respect to aileron deflection are obtained from this model.

To obtain sideslip and rudder control derivatives, a third model was used. The vertical surface was described in the X-Y plane, as shown in figure 1(c). Angular changes in the X-Z plane, which would usually be considered angle of attack, represent sideslip to this model. The asymmetric option was used.

The horizontal surfaces, as well as the fuselage, were not included because their effect on the directional derivatives is small. On some aircraft the fuselage should be included in the determination of the directional derivatives, although on the TACT aircraft the fuselage is distributed evenly about the center of gravity. Because the coordinate axis system has been rotated 90° for this model, forces in the Z direction labeled C_N correspond to side forces on the vertical tail, and moments labeled C_m represent yawing moments. Using this analogy, sideslip and rudder control derivatives can be obtained.

Some of the TACT stability and control derivatives determined with the Wing-Body program are shown in figure 2. Corresponding flight data are also shown.

The results are for Mach 0.6 flow with the wings swept to 26° . In general, the correlation between Wing-Body and flight data is good.

The longitudinal derivatives in figure 2(a) demonstrate good agreement up to an angle of attack of 7° . Flow separation is expected above this angle of attack. The predicted elevator control derivatives in figure 2(b) are generally higher than experimental values. A contribution to this derivative that is not accounted for by Wing-Body is the decrease in dynamic pressure in the wing wake.

The aileron control derivatives in figure 2(c) are computed with respect to differential deflection of the rolling tail surfaces. Yawing moment due to aileron deflection, $C_{n_{\delta_a}}$, from both flight and computed data is very small. The Wing-

Body results are computed neglecting the vertical tail. For this reason, flight data yield slightly proverse yaw while Wing-Body predicts slightly adverse yaw. Results for rolling moment due to aileron deflection, $C_{l_{\delta_a}}$, correlate well.

The predicted yaw and roll moment derivatives with respect to rudder deflection (fig. 2(d)) also show good correlation with flight data.

A similar stability and control analysis has been made of the AD1 oblique wing research vehicle at various asymmetric wing sweep angles. The results were used to verify the design and procure the airplane.

FLOW FIELD DETERMINATION

Wing-Body has been used to estimate the potential flow direction in front of an aircraft in subsonic flow and to identify nonpotential flow in flight data. Examples of each of these studies will be discussed.

The upwash angle created forward of the TACT wing was calculated using Wing-Body. The computer model includes the TACT aircraft planform as well as a small fictitious wing panel located a few centimeters forward of the TACT wing's leading edge. By making the fictitious panel sufficiently small, its effect on the flow field around the TACT airplane can be neglected. The ΔC_p value of this panel will be calculated with the effect of the TACT upwash field. A second computer pass was required to determine the lift characteristics of the fictitious panel without the influence of the TACT aircraft. The differential pressure coefficient of this panel is shown as a function of angle of attack for both of these computer runs in figure 3. The increase in ΔC_p due to the presence of the TACT planform is a function of the upwash angle. For any given ΔC_p value, the difference in angle of attack between the two curves is equal to the upwash angle. This technique has also been used to suggest angle of attack vane corrections for the highly maneuverable aircraft technology (HiMAT) and A-10 aircraft.

Another use of the Wing-Body program has been to identify nonpotential flow when it appears in experimental data. By obtaining a good potential theory pressure solution using Wing-Body, nonlinear flow effects will be absent. Comparable data taken in flight may include vortex, separated, or other flow effects. When flight and potential pressure values are compared, nonlinearities in the flight data become clear.

The formation of the leading edge vortex on the wing glove region of the TACT aircraft was identified by comparing the flight-measured and calculated potential pressure values. The Wing-Body model used for this study is shown in figure 4. The distribution of panels was heavily concentrated near the wing root to improve the accuracy of the pressure values computed in this region. Experimental pressure data were obtained from the full-scale TACT aircraft. Pressure orifices were located in the wing glove region, and measurements were taken primarily as a function of angle of attack.

The results from flight and from the potential solution are compared in figure 5. At low angles of attack it is obvious that the potential theory provides a close approximation of the measured pressure values. As the angle of attack is increased above 6° , some nonlinear effects in the flight data become evident. Experience suggests the formation of a vortex at this condition, which produces the nonlinear divergence from the potential solution.

LAUNCH DYNAMICS

Using the Wing-Body technique, an analytical study of the proposed X-24C National Hypersonic Flight Research Facility launch dynamics was performed. The X-24C aircraft was intended to be carried to a suitable launch altitude by the B-52 airplane and then released. The interference effects of the B-52 airplane on the X-24C stability derivatives during such a proposed launch were calculated. Changes in pitching moment, rolling moment, and lift as a function of the vertical separation between the two vehicles was of primary interest. Also, as a part of this study, changes in the X-24C design, pitch angle, and launch pylon position were analyzed. Changes in control effectiveness were not determined; however, these, as well as the effects of X-24C roll attitude, could also have been studied using the Wing-Body program.

Various X-24C designs were modeled with both wing and body panels. To insure that an adequate computer model had been obtained, the X-24C aircraft was first analyzed without the influence of the B-52 carrier aircraft. Wind tunnel data were available for one design, and they are compared with Wing-Body results in figure 6. Good correlation is shown between the experimental and theoretical values of longitudinal coefficients. The Wing-Body computer model of the X-24C aircraft was then used as part of the mated configuration model similar to that shown in figure 7.

Because this program allows only one aircraft fuselage to be modeled, the B-52 aircraft was represented by a wing surface only. A separate set of computer passes was made to determine the camber for this wing surface so that the model would include the effect of the B-52 fuselage on the lift distribution. First, the B-52 aircraft was modeled with both wing and body panels. The resulting ΔC_p

values on the right wing were used as the input for a subsequent computer pass. A design option, which is available from Wing-Body, was used to compute the camber values required to produce a given ΔC_p distribution. For this model, the fuselage and left wing were eliminated. Using the camber values generated by this computer pass, the right wing panels produced the same loading both spanwise and chordwise as the complete B-52 configuration.

The B-52 and X-24C models were then combined geometrically (fig. 7). Again it was necessary to cause the streamwise panel edges to align at common span stations. The configuration in figure 7 shows the X-24C aircraft in the mated position with only 0.3 meter of clearance between its fuselage and the wing of the B-52 aircraft. The X-24C fuselage centerline had to remain in the $Z = 0$ plane due to the program's input arrangement. Therefore, to simulate an increase in vertical separation distance between the two vehicles, the Z -coordinates of the B-52 wing had to be increased.

To obtain the effects of angle of attack on the X-24C aircraft, the angle of attack of the B-52 aircraft had to remain constant. When the angle of attack input parameter is used, the angle of attack of both the X-24C and B-52 models is increased. To maintain a constant angle of attack for the B-52 wing, the camber values for the wing panels had to be reduced by the same amount as the angle of attack input parameter.

To obtain the X-24C stability terms, it was necessary to sum the panel forces externally to the Wing-Body program. The summation of panel forces performed automatically by Wing-Body would include the lift and moments generated by the B-52 wing. Therefore, the following equations were used to total the X-24C aircraft's lift, roll, and pitch coefficients.

$$C_L = (C_L)_{\text{BODY}} + \frac{1}{S} \sum_{n=1}^K (\Delta C_p)_n A_n$$

$$C_\ell = (C_\ell)_{\text{BODY}} + \frac{1}{Sb} \sum_{n=1}^K (\Delta C_p)_n A_n (YC)_n$$

$$C_m = (C_m)_{\text{BODY}} + \frac{1}{Sc} \sum_{n=1}^K (\Delta C_p)_n A_n (XC)_n$$

where K is the number of X-24C panels. A brief FORTRAN computer program was used to perform this summation using punched cards of ΔC_p values generated directly by Wing-Body.

Results obtained using the configuration shown in figure 7 are given in figure 8. Data for two launch separation distances are shown: the mated position and the position after the X-24C aircraft has descended half the distance of the B-52 wing chord. The influence of the B-52 aircraft on the X-24C aircraft drops off quickly as the separating distance increases. At higher separation distances, the characteristics of the X-24C aircraft resemble the isolated X-24C results.

As well as providing these types of data, other aspects of a proposed X-24C launch were studied. The span station at which the X-24C aircraft would be attached was varied, and the results are shown in figure 9. Only small differences were observed.

LOADS DUE TO WAKE VORTEX UPSETS

The forces and moments created by trailing wake vortices can be predicted using the Wing-Body program. Velocity components in the atmosphere that are normal to the flightpath of an aircraft can be simulated in the computer model of the vehicle. The value of a vertical velocity component when related to the airspeed of the trailing vehicle determines an additional increment of angle of attack at the corresponding region of the wing. The vertical velocity, which varies across the span of the trailing aircraft, can be effectively approximated by modeling wing twist in the trailing aircraft. The value of the induced twist angle, ψ , is derived as follows.

$$\psi = \tan^{-1} (V_z/V)$$

A wake-vortex-induced angle of attack can be calculated for each streamwise row of panels of a trailing aircraft computer model. Therefore, the computed trailing aircraft forces and moments will include the effects of the vertical airflow.

The rolling moment, C_l , created on a trailing aircraft in the wake of a B-747 jet transport was predicted using this method. The effective twist of the trailing aircraft computer model was determined from a velocity profile of the B-747 wake vortices, which were obtained from flight experiments. This B-747 wake vortex velocity profile is shown in figure 10(a).

The rolling moment created on a trailing aircraft flying in such a flow condition varies with its location in the vortex; however, the maximum rolling moment is created when the trailing aircraft's centerline is positioned in the middle of the vortex. In addition, the rolling moment produced on a trailing aircraft is a function of the planform of the trailing aircraft.

The effects of the B-747 wake vortex flow field on both a T-37 and Learjet aircraft were analyzed in this study. Computer models of the two aircraft consisted of only wing panels. The fuselages were neglected because of their small contribution to the rolling moment coefficients. The horizontal tail surfaces were not modeled because the flow field around these surfaces is dominated by the downwash of the wing. The T-37 wing is generally rectangular, while the Learjet wing has a 6.5-percent greater span, a 15.5° leading edge sweep, and a taper ratio of 0.51. Both computer models were divided spanwise into 10 rows of panels. For each streamwise row of panels, a vortex-induced angle of attack was calculated based on the B-747 flight data shown in figure 10(a) and a trailing aircraft velocity, V , of 96 m/sec. The effective twist angles produced by the peak vortex velocities were about 10°.

The results are given in figure 10(b). The rolling moment of the T-37 aircraft dropped off quickly as the aircraft moved away from the vortex core. Also, the maximum rolling moment created on the Learjet aircraft was lower than that created on the T-37 aircraft.

This study allowed an analytical comparison of two aircraft planforms subjected to an identical vortex flow field. In flight, it would be impossible to recreate a specific velocity profile for different trailing aircraft. Also, it would not be safe to subject some aircraft to such a wake vortex upset experimentally.

CONCLUDING REMARKS

Through experience gained at DFRC in the application of the Wing-Body aerodynamic analysis program, several investigations of aircraft characteristics have been made analytically. Examples of the following studies have been presented:

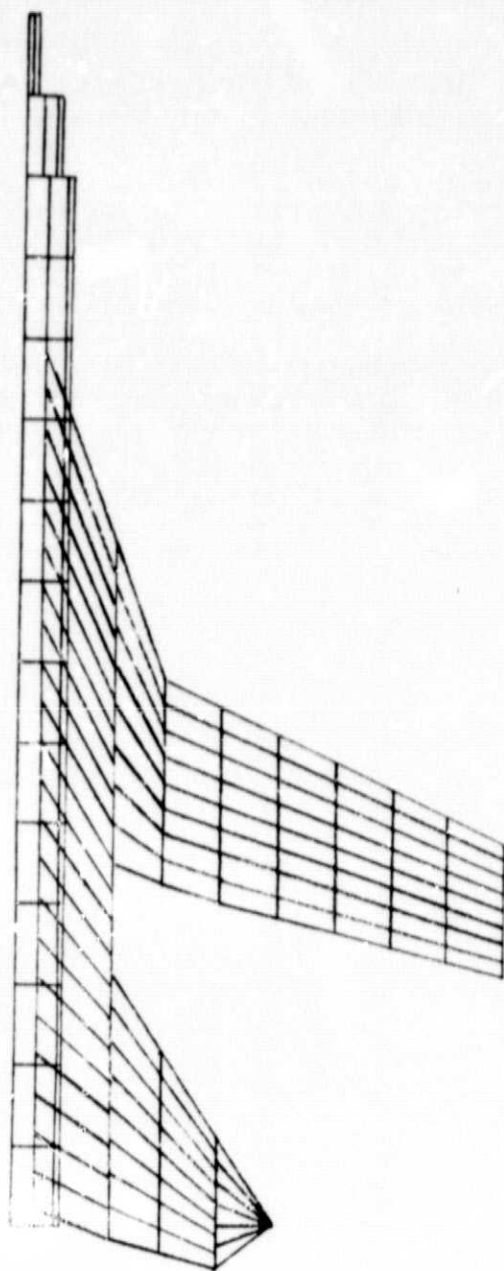
1. Determination of aircraft stability derivatives with respect to angle of attack, angle of sideslip, and control surface deflection.
2. Determination of the upwash angle in front of an aircraft.
3. Identification of the effects of nonpotential flow in experimental data.
4. Determination of interference effects of a carrier aircraft on an air-launched vehicle.
5. Determination of the loading produced on an aircraft by wake vortex flow.

Based on comparisons with experimental data presented in this report, Wing-Body analytical results may be considered reliable. Results have been used to plan wind tunnel or flight testing, or as verification of experimental work. Some situations that cannot be investigated readily or safely by experiment can be studied analytically using Wing-Body.

*Dryden Flight Research Center
National Aeronautics and Space Administration
Edwards, Calif., October 4 1978*

REFERENCES

1. Woodward, Frank A.: Analysis and Design of Wing-Body Combinations at Subsonic and Supersonic Speeds. J. Aircraft, vol. 5, no. 6, Nov.-Dec. 1968, pp. 528-534.
2. Gustavsson, S. Anders L.: A Computer Program for the Prediction of Aerodynamic Characteristics of Wing-Body-Tail Combinations at Subsonic and Supersonic Speeds. Part 2. Report AU-635, Flygtekniska Försöksanstalten (The Aeronautical Research Institute of Sweden), 1972.
3. Sim, Alex G.; and Curry, Robert E. Flight-Determined Stability and Control Derivatives for the F-111 TACT Research Aircraft. NASA TP-1350, 1978.

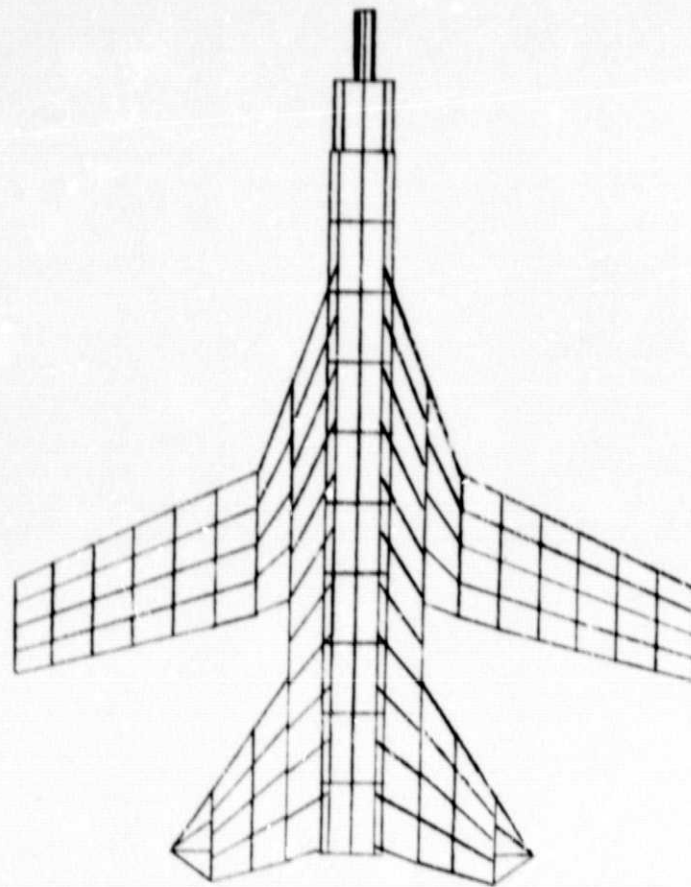


(a)

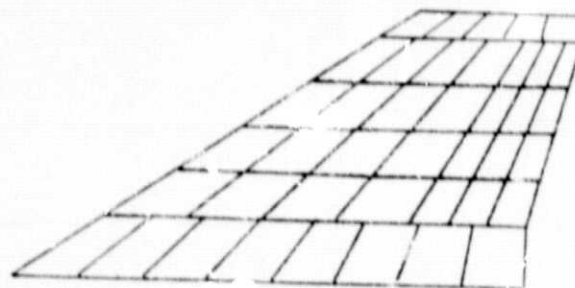
ORIGINAL PAGE IS
OF POOR QUALITY

Figure 1. Computer models for the stability and control analysis of the TACT airplane. Leading edge sweep = 25° .

ORIGINAL PAGE IS
OF POOR QUALITY

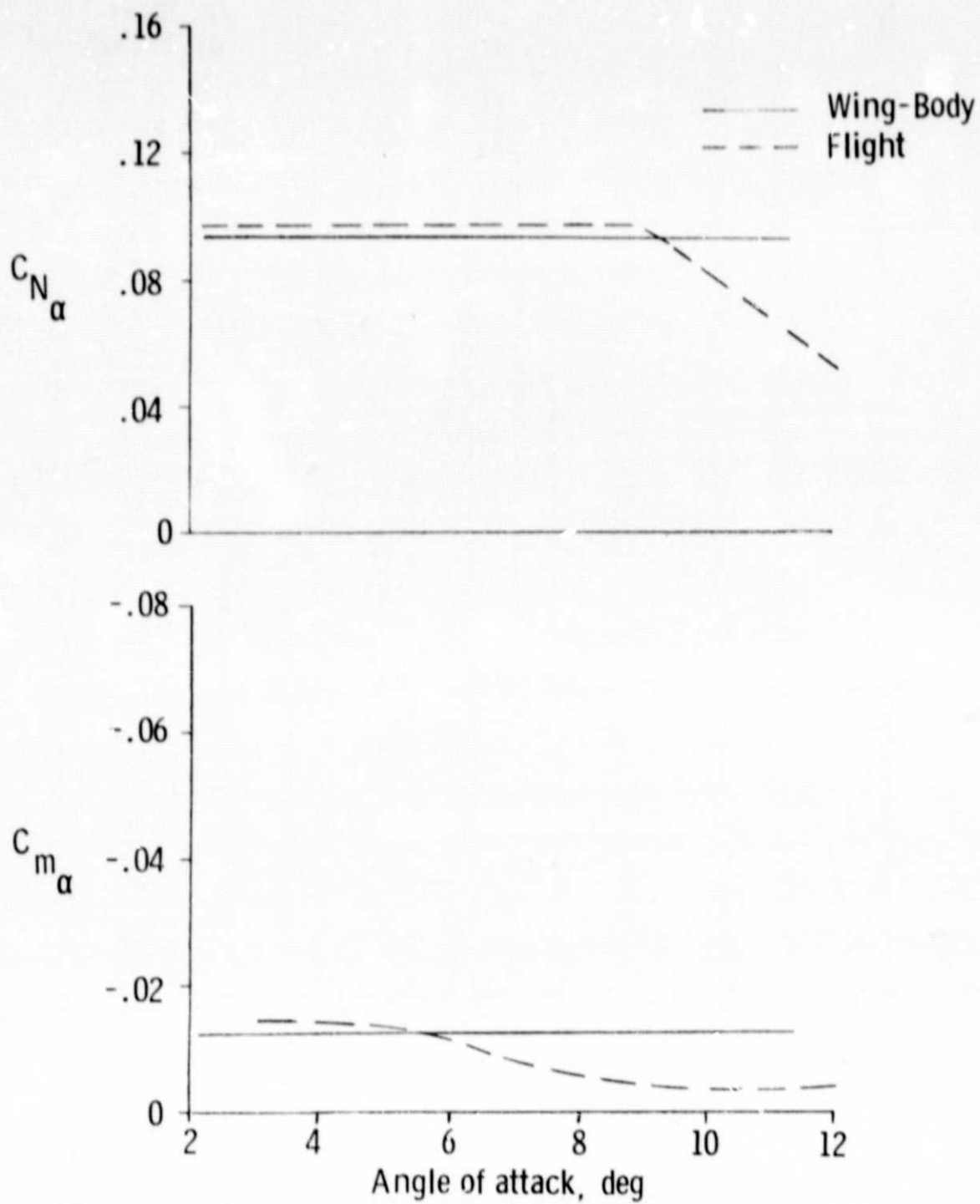


(b)



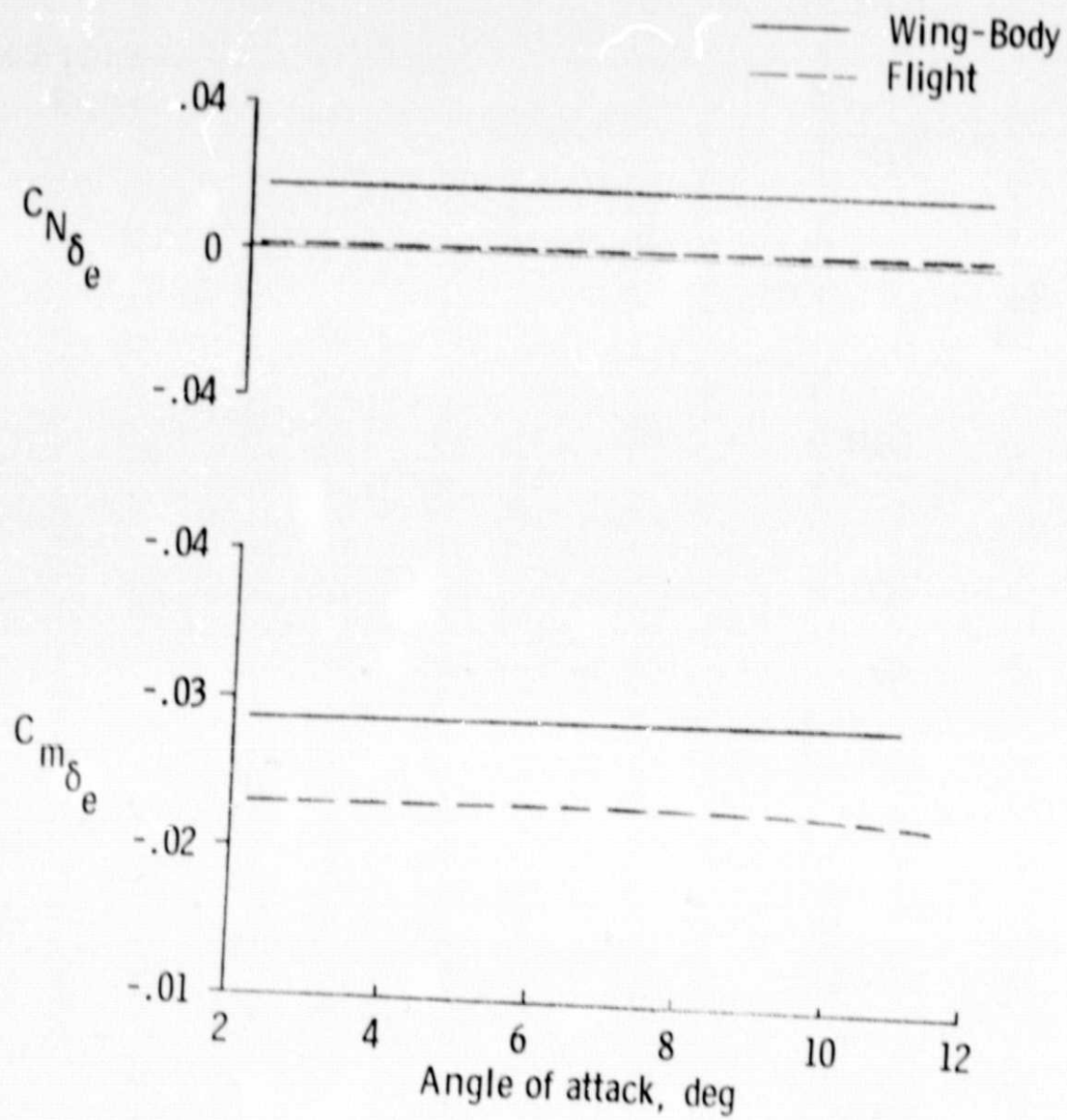
(c)

Figure 1. Concluded.



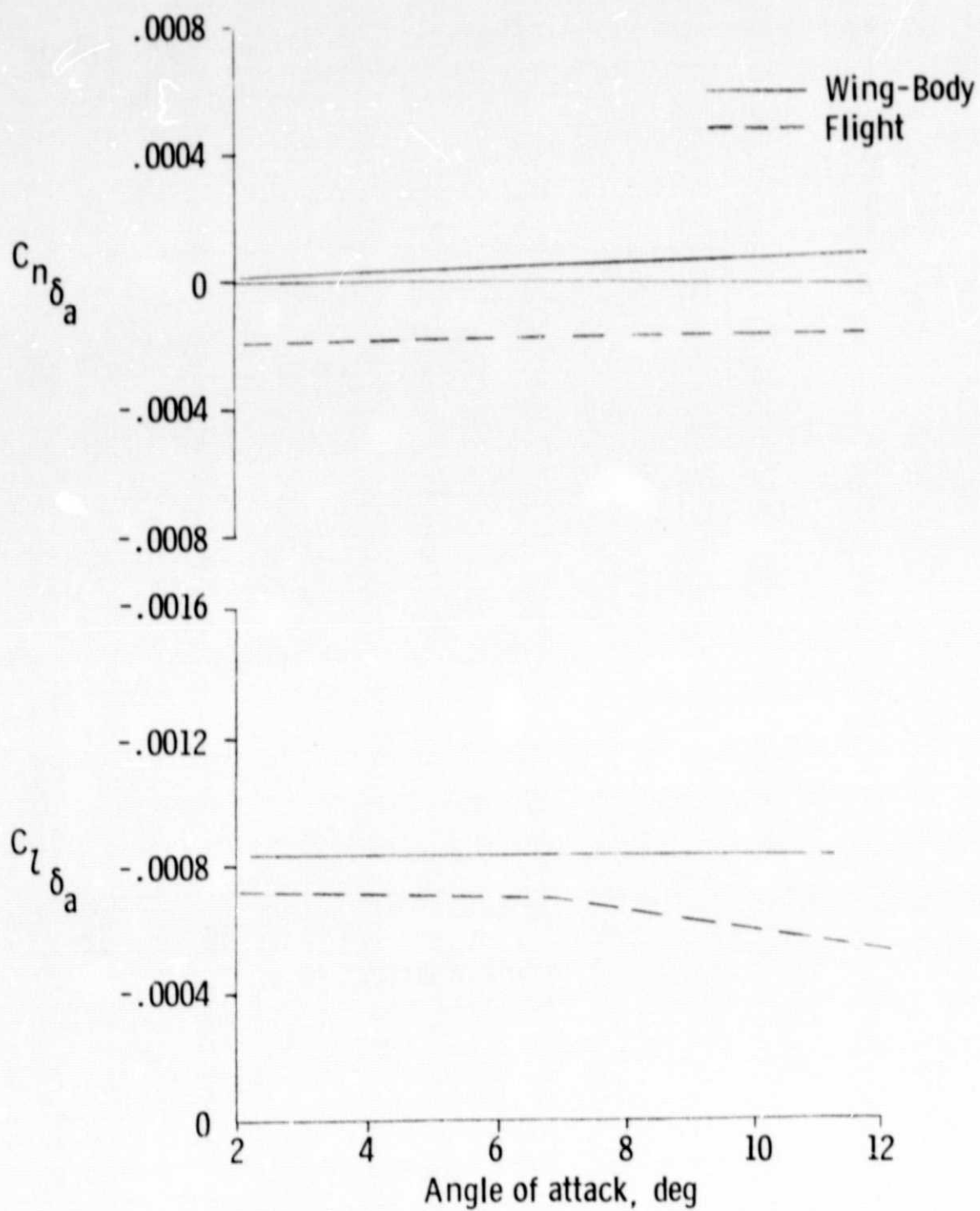
(a) C_{N_α} , C_{m_α}

Figure 2. Comparison of Wing-Body- and flight-determined stability and control derivatives.



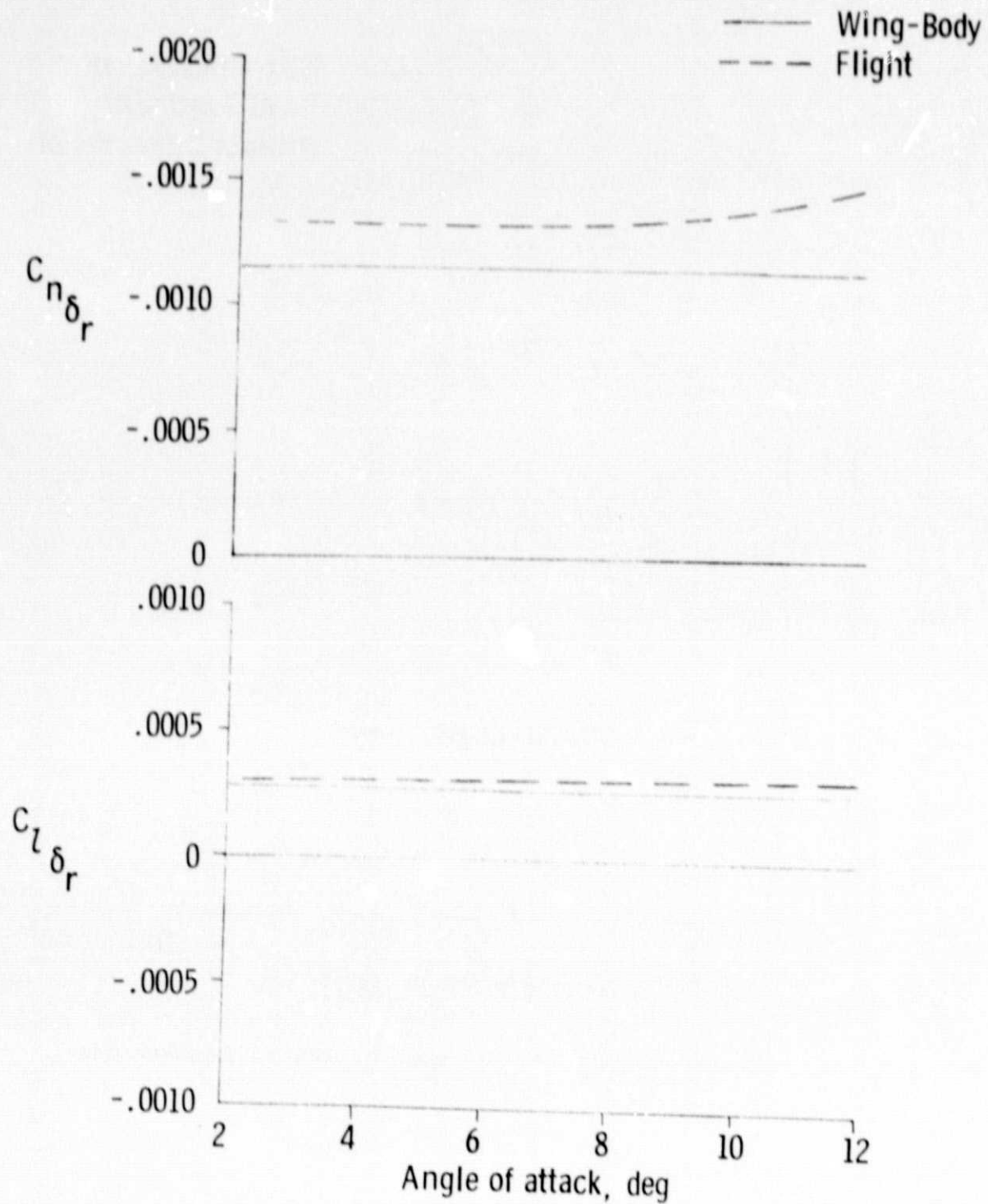
(b) $C_{N_{\delta_e}}$, $C_{m_{\delta_e}}$

Figure 2. Continued.



(c) $C_{n\delta_a}$, $C_{l\delta_a}$

Figure 2. Continued.



(d) $C_{n\delta_r}$, $C_{l\delta_r}$

Figure 2. Concluded.

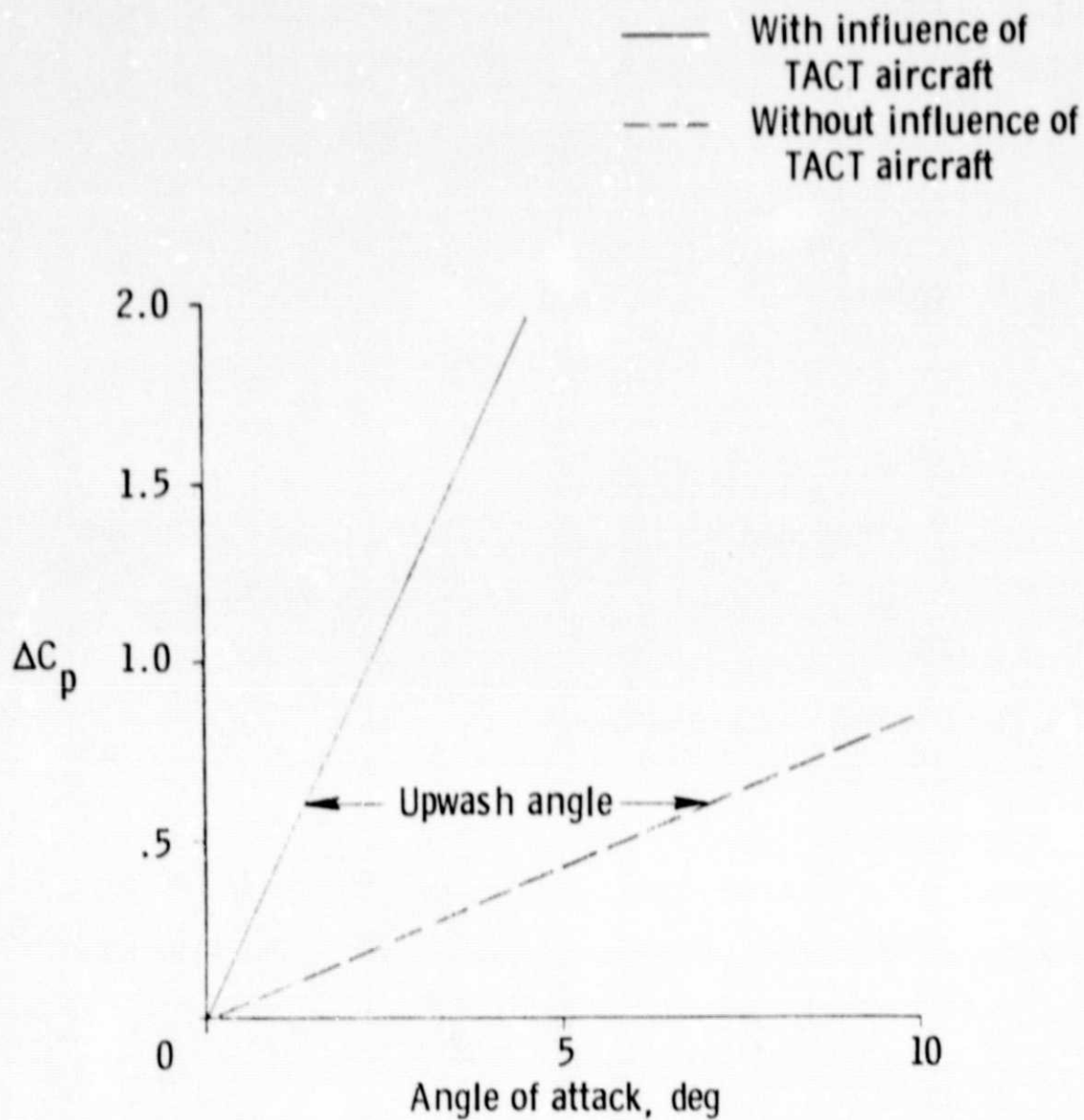


Figure 3. Pressure coefficient versus angle of attack of fictitious panel.

ORIGINAL PAGE IS
OF POOR QUALITY

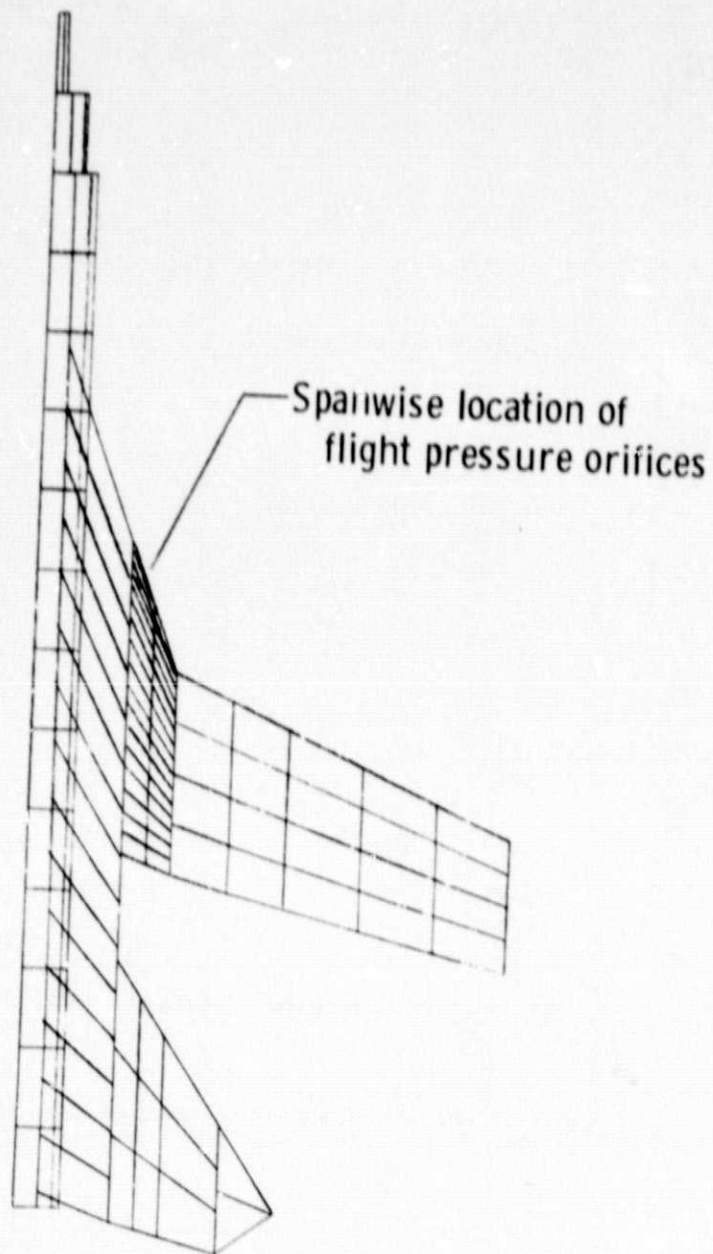


Figure 4. TACT model with concentrated paneling in the wing glove region.

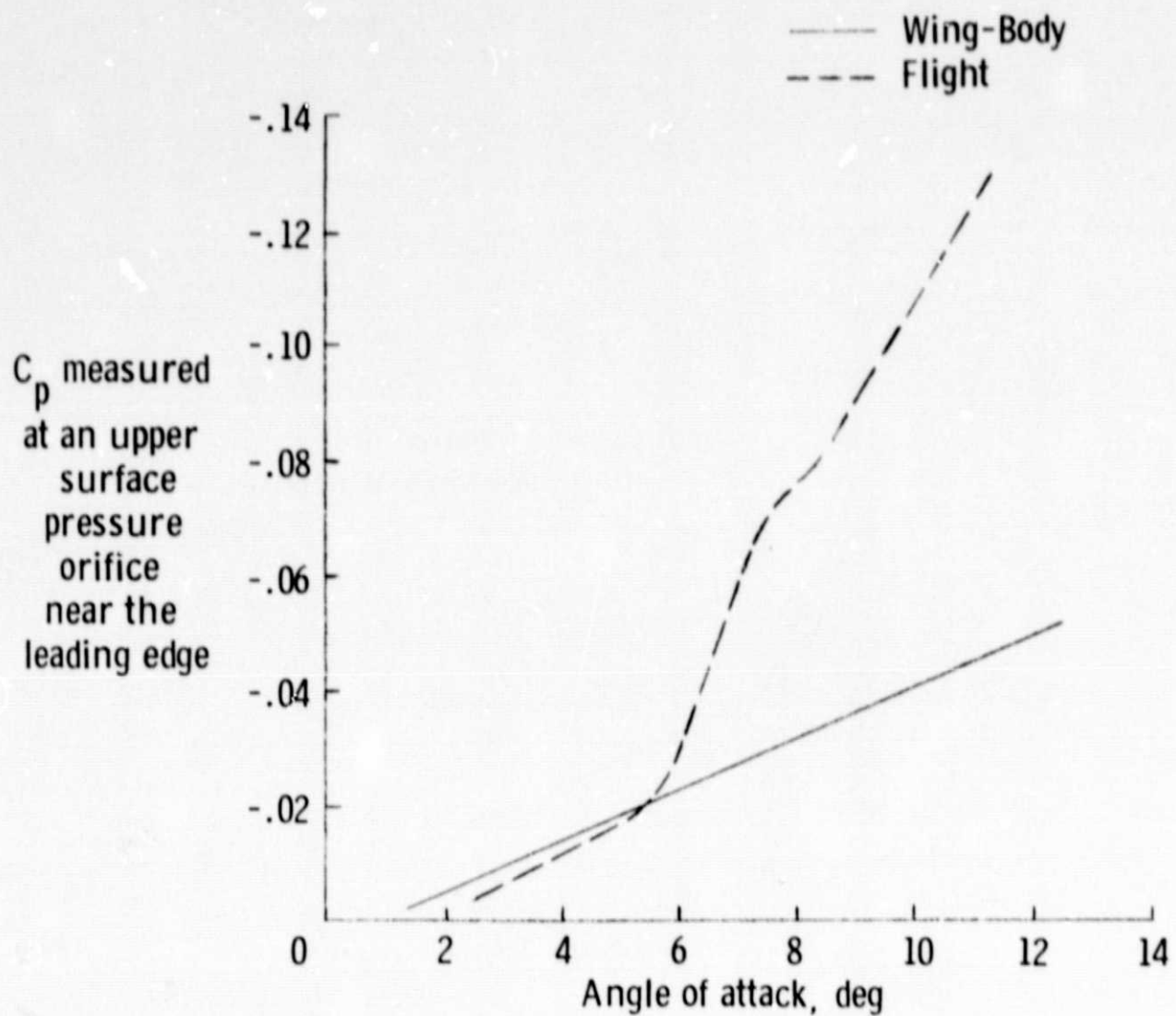


Figure 5. Comparison of potential theory results and flight data.

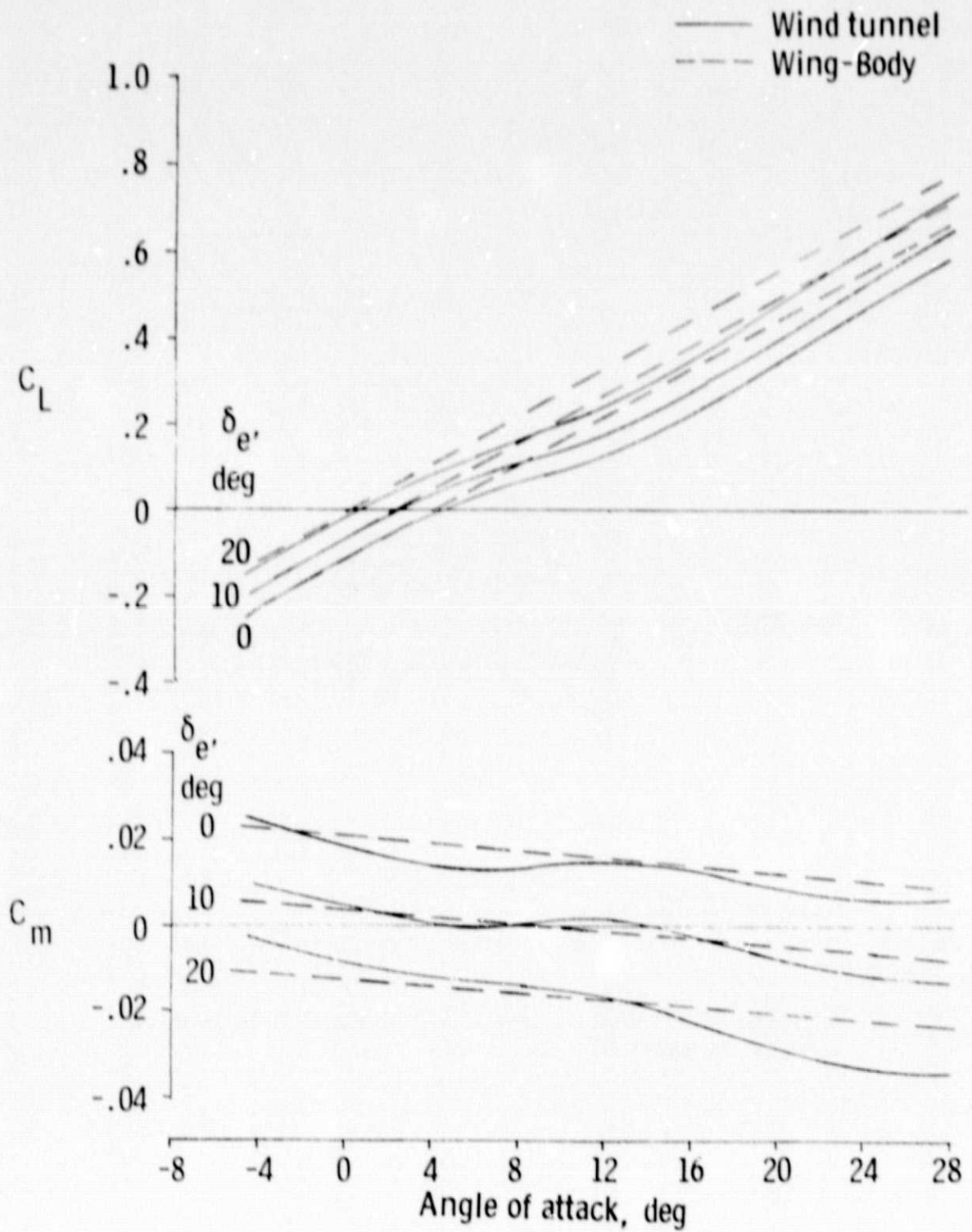


Figure 6. Isolated X-24C characteristics.

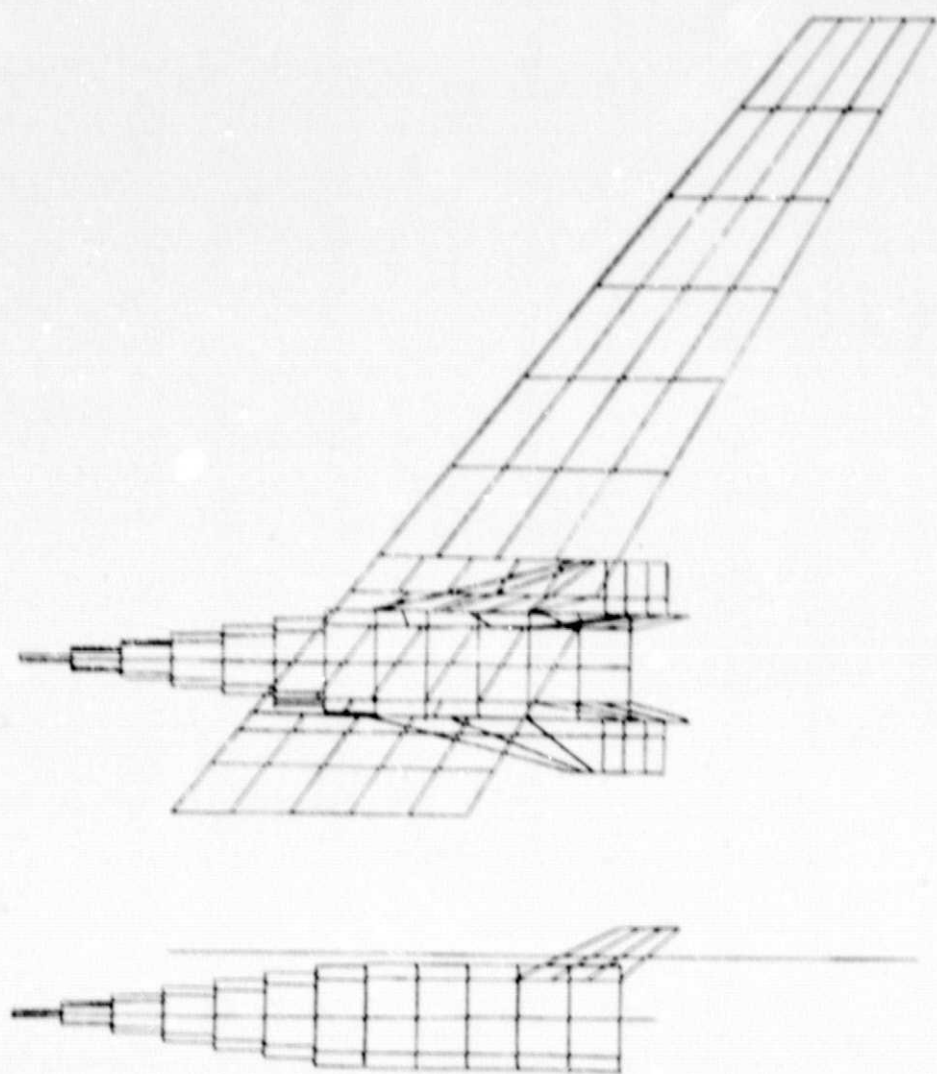
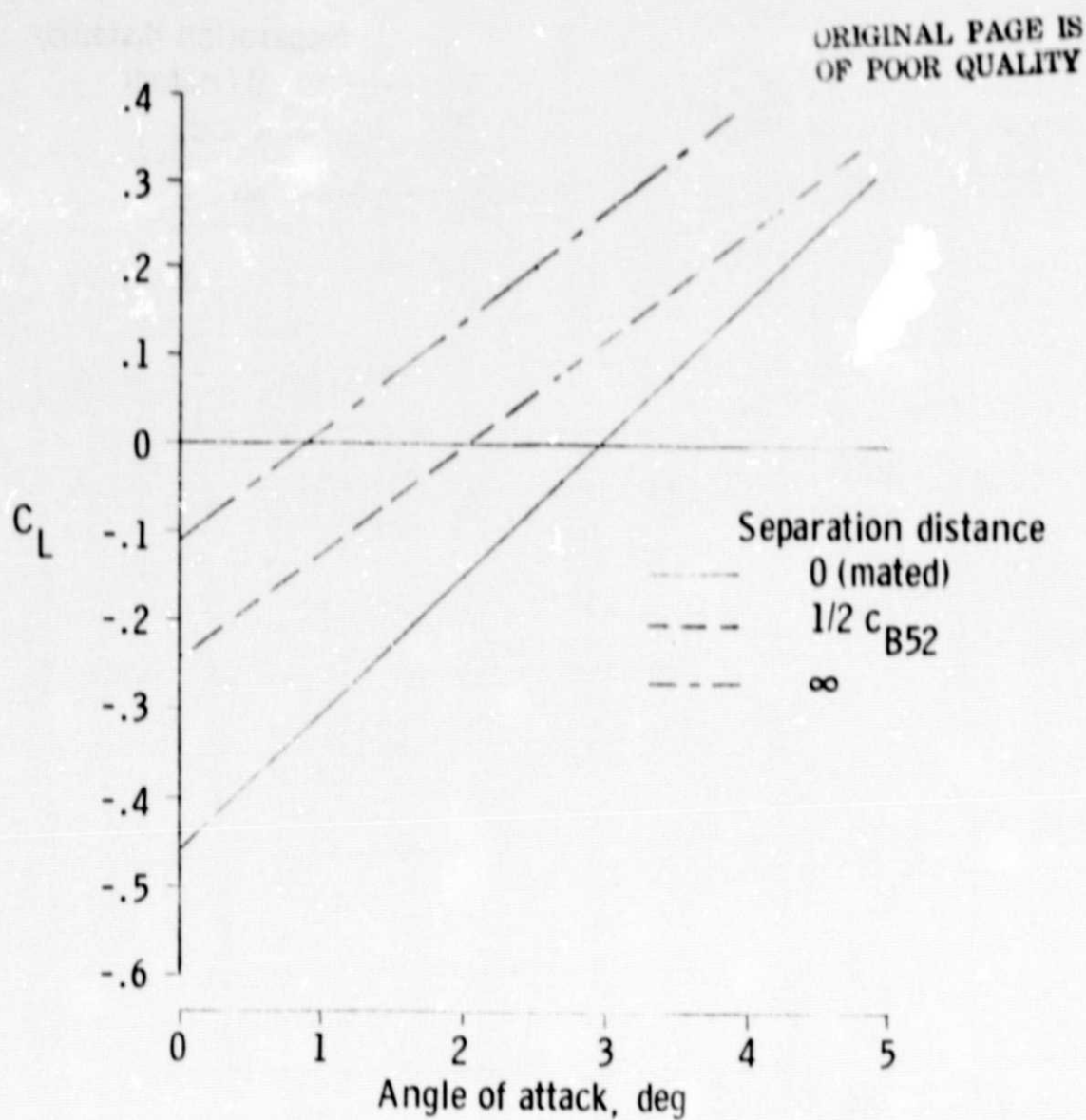
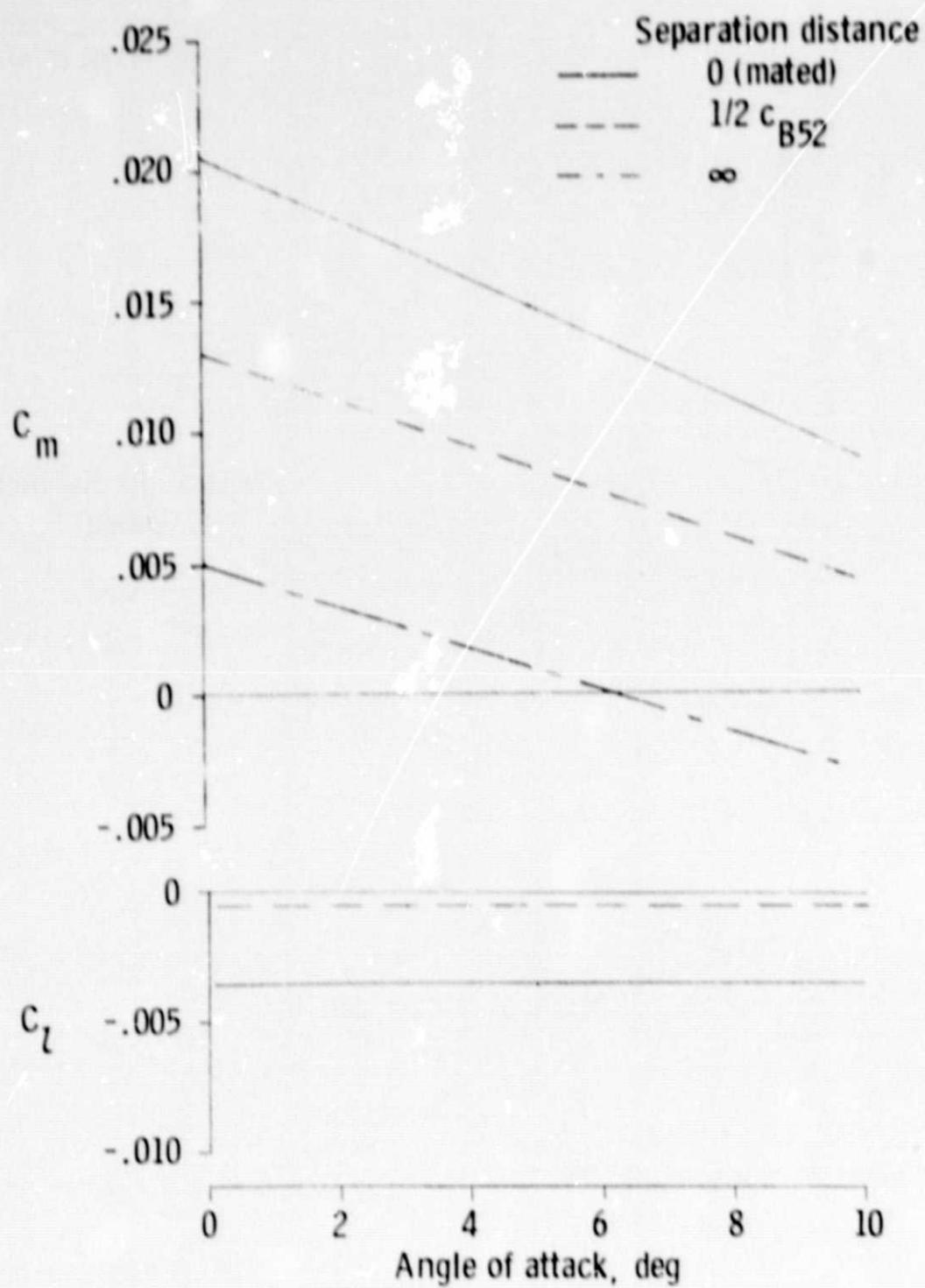


Figure 7. Computer model of X-24C and B-52 aircraft in mated configuration.



(a) C_{L_α}

Figure 8. Comparison of X-24C characteristics in presence of B-52 aircraft.



(b) C_m, C_L

Figure 8. Concluded.

ORIGINAL PAGE IS
OF POOR QUALITY

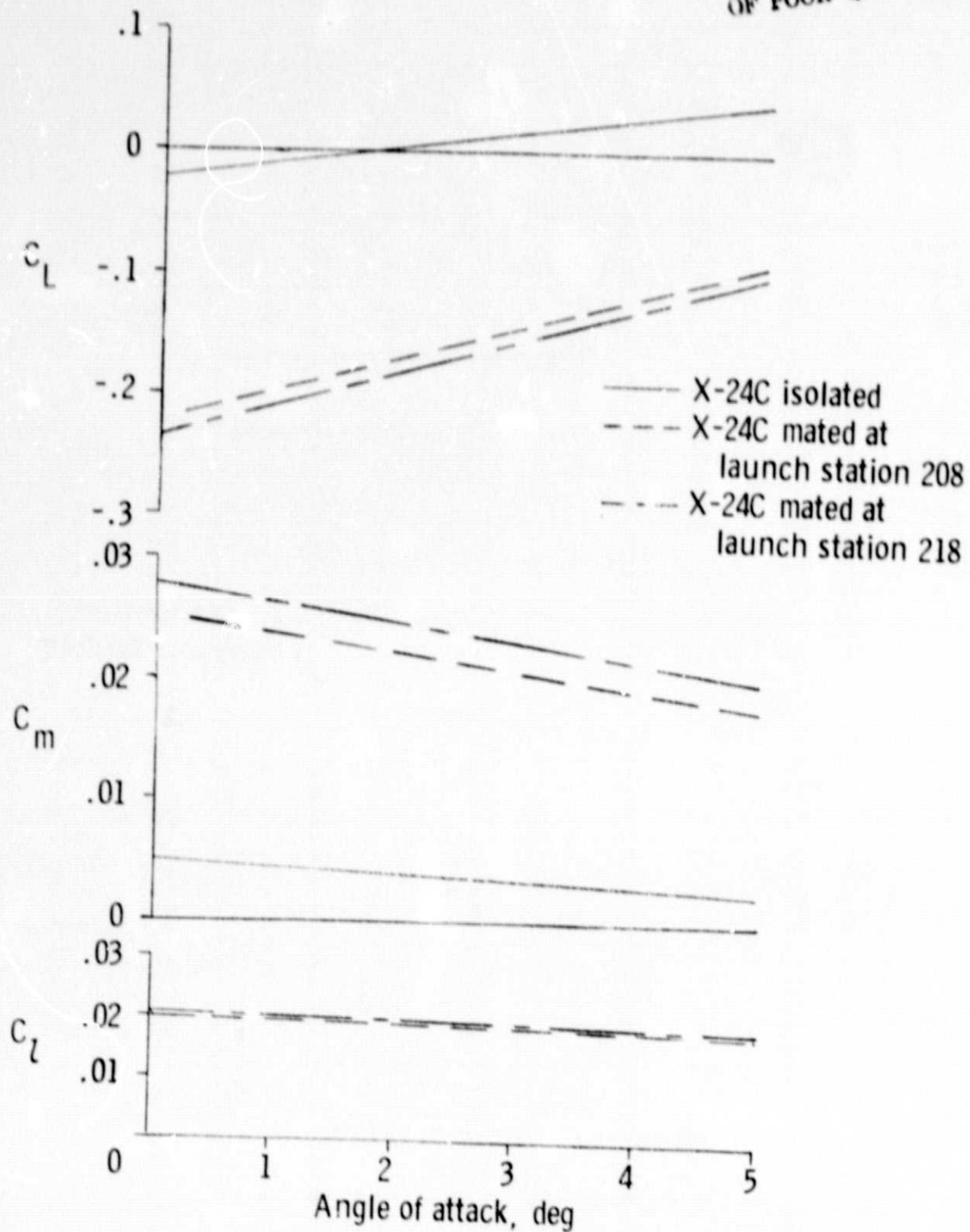
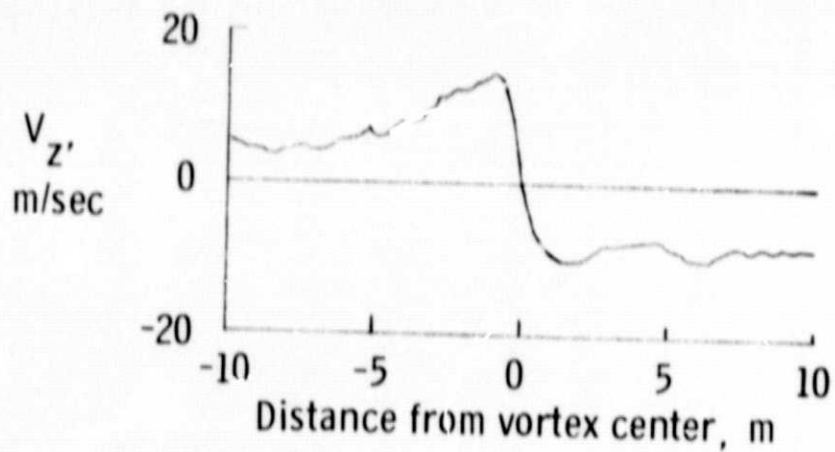
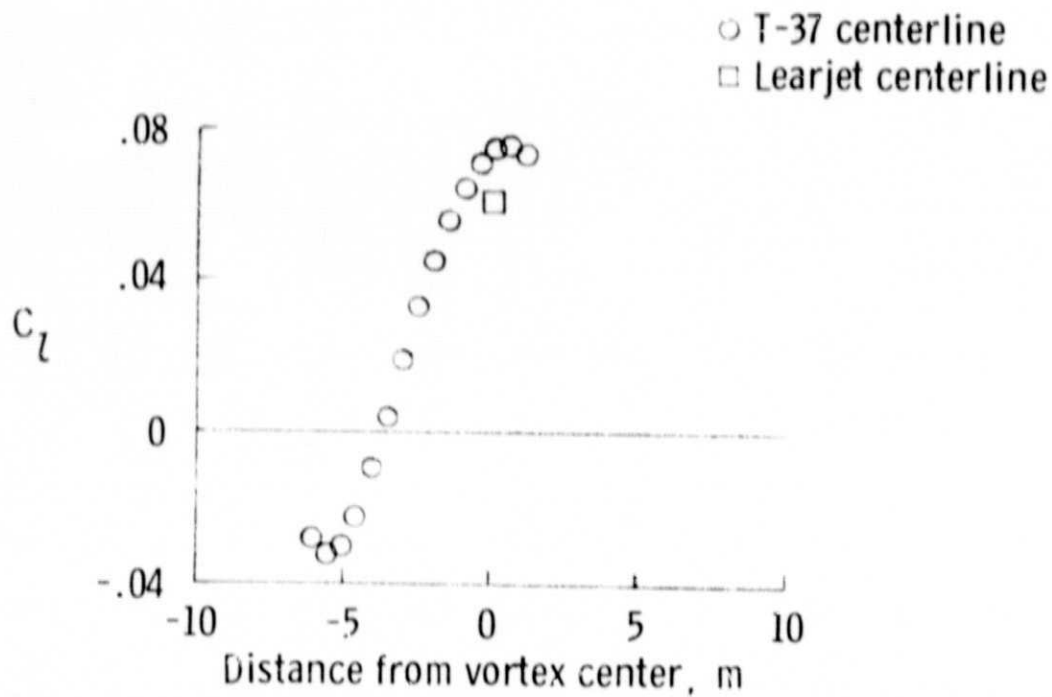


Figure 9. Comparison of characteristics of X-24C aircraft when mated to B-52 aircraft at various launch pylon positions.



(a) Velocity profile of B-747 wake vortex.



(b) C_L of trailing aircraft in vortex flow field.

Figure 10. Loads due to wake vortex study.

ORIGINAL PAGE IS
OF POOR QUALITY